

Neural Packing: from Visual Sensing to Reinforcement Learning

JUZHAN XU, Shenzhen University, China
 MINGLUN GONG, University of Guelph, Canada
 HAO ZHANG, Simon Fraser University, Canada
 HUI HUANG, Shenzhen University, China
 RUIZHEN HU*, Shenzhen University, China

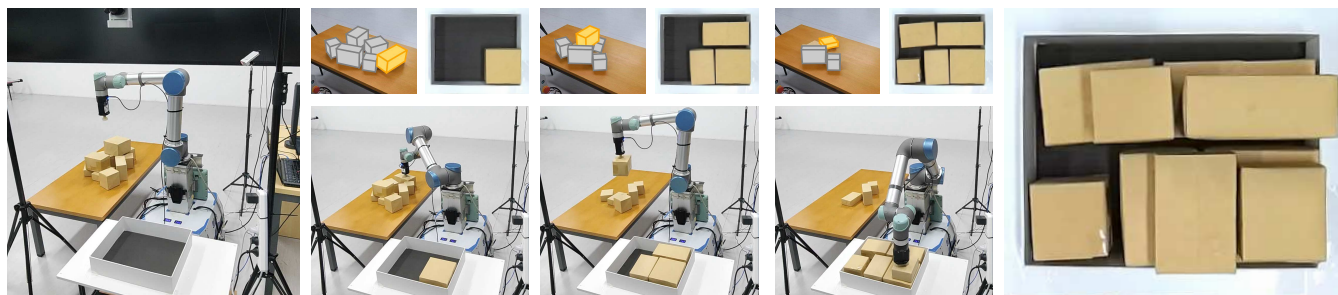


Fig. 1. We present a full solution pipeline for the 3D transport-and-packing (TAP) problem, which is based on reinforcement learning and real-time RGBD sensing of the source objects and the packing state in the target container (top row). The series of photographs show a Universal Robots UR5e robotic arm executing a TAP solution produced by our network, which simultaneously selects an object (colored in yellow) to pack and determines a final packing location.

We present a novel learning framework to solve the transport-and-packing (TAP) problem in 3D. It constitutes a full solution pipeline from partial observations of input objects via RGBD sensing and recognition to final box placement, via robotic motion planning, to arrive at a compact packing in a target container. The technical core of our method is a neural network for TAP, trained via *reinforcement learning* (RL), to solve the NP-hard combinatorial optimization problem. Our network simultaneously selects an object to pack and determines the final packing location, based on a judicious encoding of the continuously evolving states of partially observed source objects and available spaces in the target container, using separate encoders both enabled with attention mechanisms. The encoded feature vectors are employed to compute the matching scores and feasibility masks of different pairings of box selection and available space configuration for packing strategy optimization. Extensive experiments, including ablation studies and physical packing execution by a real robot (Universal Robot UR5e), are conducted to evaluate our method in terms of its design choices, scalability, generalizability, and comparisons to baselines, including the most recent RL-based TAP solution. We also contribute the first benchmark for TAP which covers a variety of input settings and difficulty levels.

*Corresponding author: Ruizhen Hu (ruizhen.hu@gmail.com)

Authors' addresses: Juzhan Xu, juzhan.xu@gmail.com, Shenzhen University, China; Minglun Gong, gongml@gmail.com, University of Guelph, Canada; Hao Zhang, haoz@cs.sfu.ca, Simon Fraser University, Canada; Hui Huang, hhzhuyan@gmail.com, Shenzhen University, China; Ruizhen Hu, ruizhen.hu@gmail.com, Shenzhen University, China.

Permission to make digital or hard copies of all or part of this work for personal or classroom use is granted without fee provided that copies are not made or distributed for profit or commercial advantage and that copies bear this notice and the full citation on the first page. Copyrights for components of this work owned by others than the author(s) must be honored. Abstracting with credit is permitted. To copy otherwise, or republish, to post on servers or to redistribute to lists, requires prior specific permission and/or a fee. Request permissions from permissions@acm.org.

© 2023 Copyright held by the owner/author(s). Publication rights licensed to ACM. 0730-0301/2023/12-ART269 \$15.00
<https://doi.org/10.1145/3618354>

CCS Concepts: • **Computing methodologies** → **Shape modeling**; *Sequential decision making*; Vision for robotics.

Additional Key Words and Phrases: packing problem, visual sensing, transport-and-pack, neural networks for combinatorial optimization, reinforcement learning

ACM Reference Format:

Juzhan Xu, Minglun Gong, Hao Zhang, Hui Huang, and Ruizhen Hu. 2023. Neural Packing: from Visual Sensing to Reinforcement Learning. *ACM Trans. Graph.* 42, 6, Article 269 (December 2023), 11 pages. <https://doi.org/10.1145/3618354>

1 INTRODUCTION

3D packing is a real-world problem in the transport and warehousing industries, with ever-increasing number of packages delivered daily. According to a study by the National Institute of Standards and Technology (NIST) in the US, packaging represents about 25% of the solid waste generated annually. Hence, improving packing efficiency has important economical and environmental impacts. On top of that, there has been a continuing drive towards robotic automation of warehouse operations including object transport and packing for improved operational continuity and worker safety, e.g., when handling heavy packages or packing in a confined space.

To date, most packing problems tackled in graphics, whether for cartification [Lévy et al. 2002; Limper et al. 2018; Nöll and Stricker 2011; Sander et al. 2003], pattern generation [Doyle et al. 2019; Kaplan and Salesin 2000], or fabrication [Chen et al. 2015; Koo et al. 2016; Vanek et al. 2014], have only focused on maximizing the efficiency of the *final packing state*. The recent work by Hu et al. [2020], TAP-Net for Transport-and-Pack, was the first to jointly account for the *transport* aspect of the problem, i.e., how to select

an object to pack and how to transport it to the target container, as both issues must be considered for physical packing.

As a first solution however, TAP-Net makes simplifying assumptions on the number, pose, and location of the source objects and resorts to heuristic packing strategies, rendering the problem setting and solution impractical and sub-optimal. Our goal in this work is to develop a learning framework which encompasses a *full TAP pipeline*, from partial observations of input objects via visual sensing to final box placement to arrive at a compact packing, without making limiting assumptions on the object or container states as in TAP-Net, except that all objects remain as *boxes*; see Figure 1.

Figure 2 shows an overview of our pipeline. Given a set of source objects stacked on a workspace, our goal is to pack the objects compactly into a target container using a robot arm with a vacuum gripper. Two RGBD cameras are employed to observe source objects and the target container, respectively, for object selection and packing strategy optimization, as shown in Figure 2(a).

With the captured RGBD images, we first analyze the current workspace and extract information important for packing, as shown in Figure 2(b). For source objects that are observable from the camera, we estimate their dimensions and further extract a *precedence graph*, which encodes the constraints on the pick-up orders among the objects. For the target container, we extract its *height map*, which is used to generate a set of *empty maximal spaces*, or EMS [Parreño et al. 2008] for short, to indicate candidate packing locations.

The technical core of our method is the packing network, coined TAP-Net++. It takes both box information and the set of candidate EMS as input, and simultaneously selects a box to pack and determines the final packing location, based on a judicious encoding of the continuously evolving states of partially observed source boxes and EMS configurations, using separate encoders both enabled with attention mechanisms (see Figure 5). The encoded feature vectors are employed to compute the matching scores and feasibility masks of different pairings of box state and candidate EMS. Finally, the pair with the highest matching score is selected to guide the packing, as shown in Figure 2(c). With the packing problem an NP-hard combinatorial optimization, which is unfitting for supervised learning due to the difficulty of collecting sufficient ground-truth data, we train TAP-Net++ using reinforcement learning (RL). Importantly, TAP-Net++ is trained for both box selection and packing into the target container, while TAP-Net only learns the former and determines the packing position separately and heuristically.

Once a box has been selected and the target packing position determined by TAP-Net++, we employ a motion planning method to generate the motion sequence for the robot arm to execute the packing. As shown in Figure 2(d), the workspace is updated accordingly to initiate the next box selection and packing.

Extensive experiments including ablation studies are conducted to evaluate our method in terms of its design choices, scalability, and generalizability. We also contribute the first benchmark for TAP which covers a variety of input settings and difficulty levels, over which we comprehensively evaluate TAP-Net++ against TAP-Net, its closest competitor. Physical packing execution by a real robot, a Universal Robot UR5e, has also been carried out to demonstrate deployment of our method in a non-simulation setting.

Table 1. Comparing various aspects of TAP-Net++ vs. TAP-Net.

	TAP-Net	TAP-Net++
Input	Virtual boxes, axis-aligned, and packed in a container	Real boxes, casually stacked, with random poses
Box config.	Known	Predicted from partial observation
# instances	Fixed	Flexible
Overall solution	Two-step optimization	One-step optimization
Network output	Packing order and state	Packing order, state, and location
Packing strategy	Heuristic: MACS	Optimized by neural network

2 RELATED WORK

In this section, we briefly mention several real-world examples of automated packing using robots to motivate the TAP problem. We then cover prior packing strategies and provide a detailed comparison between TAP-Net++ and TAP-Net [Hu et al. 2020].

Real-world robotic automation. Automating warehouse operations including order retrieval, shelving, packaging, and packing is one of the most critical innovations considered by many commercial companies including eCommerce giants such as Amazon and Walmart. At many of its fulfillment centers, Amazon employs its warehouse robots to automate picking, moving, and packing solutions. In particular, two of Amazon’s recently unveiled robotic arm cells, Cardinal and Sparrow, are designed for the transport-and-pack problem. While the main innovation of the Sparrow robot is to use its suction cups to firmly grasp and move items of varying shapes and sizes, the task carried out by the Cardinal robotic arm is the closest to ours. According to this [official Youtube video](#) from Amazon, Cardinal employs “advanced artificial intelligence and computer vision to nimbly and quickly select one package out of a pile of packages, lift it, read the label, and precisely place it in a GoCart.” However, it does not appear that the box selection or packing was optimized to arrive at a compact packing at the target containers.

Packing strategies. One strategy adopted by prior works is to traverse all possible packing positions in the container and pick the one with the highest score, where the scoring criterion may be Deepest-Bottom-Left with Fill (DBLF) [Karabulut and Inceoglu 2004] or via height map minimization [Hu et al. 2017; Wang and Hauser 2019]. Another way is to select from a set of candidate packing positions. To characterize such positions, corner points [Lodi et al. 2002; Martello et al. 2000, 2007], extreme points [Baldi et al. 2012; Crainic et al. 2008], and empty maximal spaces (EMS) [Parreño et al. 2008] have been employed. In particular, heuristic methods such as Best-Match-First (BMF) [Li and Zhang 2015] and Online Packing Heuristic (OnlineBPH) [Ha et al. 2017] have proposed suitable rules to select packing locations based on EMS. In our work, we extract a height map over the target container and generate candidate packing locations via EMS. The discretized description of the container states significantly reduces the searching space for packing.

Among the recently proposed learning-based packing strategies, Zhao et al. [2021a] designed a neural network to score all possible packing positions based on height maps over the container, while in [Zhao et al. 2021b], a hierarchical packing configuration tree is

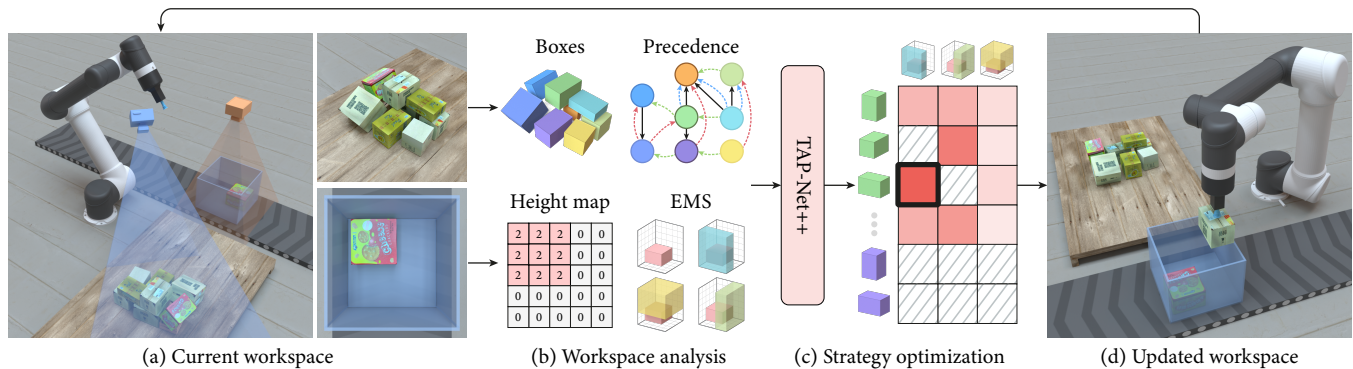


Fig. 2. Overview of our method. Given the RGBD images captured from both the source objects and the target container (a), our method starts with extracting essential information for packing optimization. This includes the dimensions of source objects and their precedence constraints, as well as the height map of the target container and candidate packing locations, referred to as EMS (b). This information is fed into TAP-Net++, which outputs a matching score for each pair of object state and candidate EMS. The pair with the highest matching score, highlighted with a thick border, is selected as the optimal packing strategy (c), i.e., the third box state will be selected and packed into the first EMS. The robot arm then picks the selected box with the desired state and packs it into the optimized position, which triggers the next iteration of object selection and packing.

learned based on EMS. Hu et al. [2020] trains a neural network, TAP-Net, to optimize the order of boxes to be packed, while resorting to a heuristic coined Maximize-Accessible-Convex-Space (MACS) as the packing strategy. MACS was designed to account for accessibility issues pertaining to future packing and to accommodate large objects. They opted to not train a separate packing network as it did not improve over their heuristic-based approach.

TAP-Net++ vs. TAP-Net. Table 1 compares TAP-Net++ and TAP-Net in terms of input, output, box configuration, and packing strategies, etc. In more detail, TAP-Net is designed to only deal with a fixed number of instances as input, and use an auxiliary rolling scheme to handle tasks with more instances. With a more advanced network architecture, TAP-Net++ affords more flexibility to the number of instances and is able to deal with dynamic inputs obtained from partial observations. More importantly, TAP-Net adopts a two-step optimization, where the network only optimizes the packing order and state of the input boxes and the final packing position of the selected box is determined by a heuristic packing strategy, which may lead to suboptimal solutions. TAP-Net++ discretizes the packing space and directly outputs the packing location, along with the parking order, through a one-step optimization.

3 METHOD

Here we discuss the two key steps of our method in more detail: the analysis of workspace state in Section 3.1 and the optimization of packing strategy in Section 3.2.

3.1 Workspace state analysis

Source objects and precedence graph. The objective of this phase is to identify objects that need to be packed and extract their precedence relations using the single-view RGBD image captured; see the blue camera in Figure 2(a). Object detection is performed using the Mask RCNN network [He et al. 2017], which is followed by the estimation of dimensions and 6D pose for each object using the cuboid fitting algorithm [Jiang and Xiao 2013]. We allow the robot

arm to grasp each box object along its three axes, and possibly rotate it by 90° before packing into the target container. Consequently, there are six distinct packing states for each object; see Figure 3(a).

For a given box, certain packing states may not be accessible to the robot arm due to obstructions caused by other boxes. Thus, it becomes essential to extract a precedence graph that captures the relationships between the boxes. Inspired by the approach proposed in [Hu et al. 2020], we assign each box as a graph node, and directed edges represent different precedence relations among the boxes. However, unlike the assumption made in [Hu et al. 2020] where all source objects are assumed to be axis-aligned and initially packed in a container, we allow the objects to be casually stacked in the workspace with random poses that may not be axis-aligned. Hence, the extraction of precedence relationships becomes more complex.

More specifically, we define two types of precedence: one is Movement Block (MB), indicating the movement of an object O_1 is blocked by another object O_2 since O_2 is at least partly on top of O_1 ; the other is Access Block (AB), which indicates one of object O_1 's surfaces cannot be reached by the robot arm due to another blocking object. Based on the direction of the surface that are blocked, AB can be further divided into XAB, YAB, and ZAB, where X, Y, Z axes are randomly determined for each box during the cuboid fitting step. Since a box can be picked up from either side for a given direction, we store the blocking side of each AB edge. Then O_1 can be picked up from its X (or Y/Z) axis direction as long as there is no MB edge and at least one side of O_1 that is perpendicular to X (or Y/Z) axis direction has no XAB (or YAB/ZAB) edges pointing to it.

Figure 3 shows the process of precedence extraction on an example scene with three stacked boxes. To determine Movement Blocks, we project all the boxes from the top and check whether the projections of each pair of objects are overlapped as in Figure 3(b). If so, an MB (black) edge from the object on top to the one on bottom is added; see the three MB edges in Figure 3(c). For Access Blocks, we check whether the robot arm has access to the two surfaces along each axis direction. As shown in (a), the blue gripper along

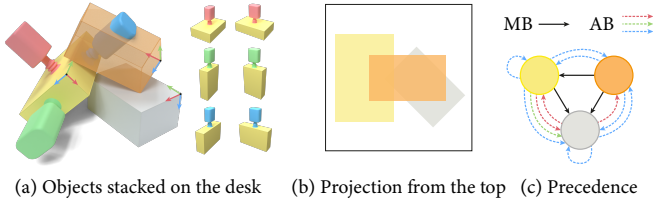


Fig. 3. Precedence extraction. (a) Example scene with three objects stacked on the desk, where the assigned X, Y, Z directions are shown in red, green, blue arrows. Grippers picking the yellow box along three directions are shown on the left, whereas all six possible packing states are shown on the right; (b) Projection of the scene from the top for MB edge detection; (c) The final precedence graph of the example scene, where MB edges are shown in black solid arrows and AB edges for different directions are shown in dashed arrow with different colors.

the local z-axis of the yellow block is blocked by the orange box. Hence a ZAB (blue dashed) edge is added from the orange to the yellow nodes; see Figure 3(c). Moreover, since the bottom of the yellow box is inaccessible, a ZAB edge from the yellow node to itself is also added. Other precedences can be derived in a similar way and the full precedence graph of this example is presented in (c).

Suppose we have detected n objects denoted as $\{O_i\}_{i=0}^{n-1}$ in the current workspace. The extracted precedence information for each object O_i can be represented as $P_i = [p_i^M, p_i^{XA}, p_i^{YA}, p_i^{ZA}]$, where $p_i^M \in \{0, 1\}^n$ indicates whether there is an MB edge pointing from each of the n objects to O_i and $p_i^{\{X/Y/Z\}A} \in \{0, 1\}^n$ indicates $\{X/Y/Z\}$ AB edge pointing to O_i along one of O_i 's local axes.

During the packing process, we need to simultaneously decide which object to pack next and its orientation in the target container, i.e., the object's packing state. Hence, we extend the precedence information to the packing state level, represented as $\{p_{6i+s}\}$, where $s \in [0, 5]$ corresponds to each of the six distinct packing states shown in Figure 3(a). Depending on the packing state s , the accessibility of object O_i depends on p_i^M and only one of $\{p_i^{XA}, p_i^{YA}, p_i^{ZA}\}$. This is because whether O_i can be picked up and packed along one of its axes is not affected by access blocks along two other axes. Therefore, we set packing state precedence $\{p_{6i+s}\} = [p_i^M, p_i^{sA}] \in \{0, 1\}^{2 \times n}$, where p_i^{sA} is the AB precedence corresponding to the direction of packing state s .

Finally, to fully encode all information associated with object O_i 's packing state s , a 3D vector $b_{6i+s} \in \mathbb{R}^3$ is used to store the dimension of O_i under the orientation specified by state s . Basically, b_{6i+s} indicates the minimum empty space needed in the target container to pack O_i along orientation s . b_{6i+s} and p_{6i+s} together form the inputs to the source (object) encoder, i.e., $B_{6i+s} = [b_{6i+s}, p_{6i+s}]$. To simplify the representation on the following packing strategy discussion, we reindex all the object states as $\{B_j\}_{j=1}^N$, where $B_j = [b_j, p_j]$ and $N = 6n$ represents the total number of object states.

Target container and EMS. Our goal here is to generate a set of candidate locations for packing based on the current container state. This is achieved through computing candidate empty maximal spaces (EMS). EMS provides a simple yet effective placement

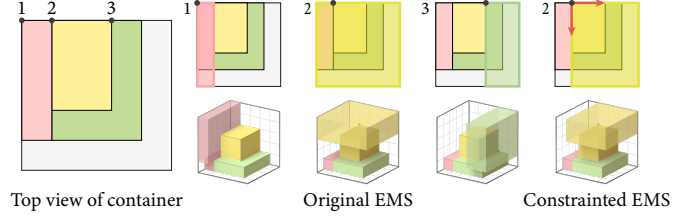


Fig. 4. Candidate EMS generation. The map on the left shows the top view of the container, with three representative top-left corners found on the map highlighted. Existing approaches compute the original EMS by expanding along all directions as shown in the middle three examples. Our approach extracts more candidate packing locations by constraining the expanding directions indicated by the red arrows, which results in a different EMS for the same corner #2. Note that due to the blocking of the tall yellow box, the constrained EMS for corner #1 and #3 is exactly the same as the original EMS.

rule, which is to align the deepest-bottom-left (DBL) corners of the selected object box and the EMS.

As shown in Figure 2(a), the camera in orange provides a single-view RGBD image of the target container. We first project the RGBD image to the local coordinates of target container to form a 2D height image, which is then discretized into a grid map to simplify candidate EMS calculation. The height of each grid is set to the maximum height of the corresponding area in the height image, resulting the grid map being axis-aligned with the local coordinate of the target container.

An EMS is defined as the largest empty orthogonal space whose size cannot extend further along the three axes [Parreño et al. 2008]. In previous approaches, EMS are only generated from a fixed corner of the container. To optimize packing, our approach considers more candidate locations through generating EMS from the left-bottom corner of each visible object; see Figure 4.

Suppose a set of candidate EMS $\{E_k\}_{k=1}^M$ is constructed, then each EMS E_k can be represented by its DBL corner $[c_k^x, c_k^y, c_k^z]$ and its dimension $[d_k^x, d_k^y, d_k^z]$. That is, $E_k = [c_k^x, c_k^y, c_k^z, d_k^x, d_k^y, d_k^z] \in \mathbb{R}^6$.

3.2 Packing strategy optimization

Different from [Hu et al. 2020], where the network only selects the object/orientation to pack and then uses heuristics to find the optimal packing position in two separate steps, we design a network to simultaneously select and pack the object in one step. This is done by finding the $\langle B_j, E_k \rangle$ pair with the highest matching score under a newly defined feasibility constraint.

Figure 5 shows the structure of our network. It can be divided into two parts: a source encoder encodes the box sizes and their precedence information into high-dimension features, and a target encoder learns the embedding of each candidate EMS. Then we multiply the features from both source and target encoders to compute the matching score and the feasibility of each pair of $\langle B_j, E_k \rangle$. The pair with the highest multiplied score will be selected as the output of the network. The box state will guide the robot to pick the selected box from the selected side and pack it at the DBL corner of the corresponding EMS in the target container. Followings, we

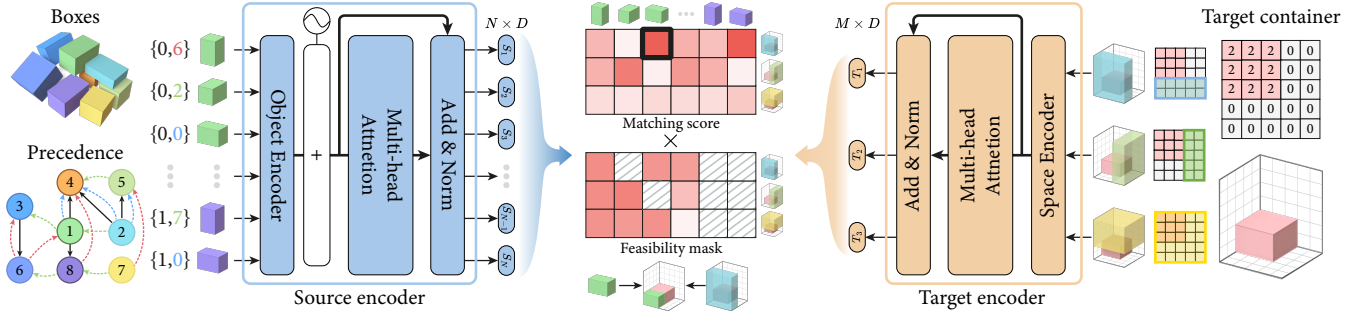


Fig. 5. Network structure of TAP-Net++. A source encoder is used to encode different box states and their precedence relations, whereas a target encoder encodes candidate EMS in the container. The feature vectors are further used to compute the matching score and feasibility mask of different (oriented box, EMS) pairs for packing strategy optimization.

give more details about each key component of our network and explain how the network is trained.

Source encoder. As shown in the source encoder module in Figure 5, taking the set of object packing states $\{B_j\}_{j=1}^N$ as input, we first extract the corresponding embedded features separately using the object encoder, and then further use an attention mechanism to extract core information in the feature map. Since the box state is order dependent in the precedence matrix, we apply a position encoding on each embedded feature before passing it to the attention mechanism. The attention module will then extract the final source object features $\{S_j\}_{j=1}^N$ with $S_j \in \mathbb{R}^D$ as output. More details about the object encoder can be found in the supplementary material.

Target encoder. For a set of M candidate EMS $\{E_k\}_{k=1}^M$ extracted in the current target container, we first use an MLP layer as the space encoder to extract features, and then use an attention module to get the final target EMS features $\{T_k\}_{k=1}^M$ with $T_k \in \mathbb{R}^D$.

Packing pair selection. Given source object features $\{S_j\}_{j=1}^N$ and target EMS features $\{T_k\}_{k=1}^M$, we compute a selection probability map $\mathcal{P} \in [0, 1]^{N \times M}$ to select the $\langle B_j, E_k \rangle$ pair with the highest probability for packing strategy optimization. In more detail, we first compute the matching score matrix $\mathcal{M} \in \mathbb{R}^{N \times M}$ with $\mathcal{M}_{jk} = \langle S_j, T_k \rangle$, where $\langle \cdot, \cdot \rangle$ represents an inner-product. We then pass both S_j and T_k through an MLP layer and get their inner product to construct the feasibility mask $\mathcal{F} = \text{sigmoid}(\mathcal{F}_{jk})$, where $\mathcal{F}_{jk} = \langle \text{MLP}(S_j), \text{MLP}(T_k) \rangle$. Note that since a box state can not be packed into a smaller EMS or may not be accessible due to precedence constraints, we further compute a corresponding validity mask $\mathcal{V} \in \{0, 1\}^{N \times M}$ to filter out invalid pairs. The final selection probability map is then defined as $\mathcal{P} = \text{softmax}(\mathcal{M} \odot \mathcal{F} \odot \mathcal{V})$, where \odot represents the element-wise product.

Note that in some cases, a box to be picked up may have its sides occluded by other boxes from the viewpoint of the source camera. Hence the estimated dimensions may not be accurate, which could lead to improper packing decisions. To address this issue, we always reevaluate the dimensions of an object after it is picked up by the robot but before it is packed into the target container. If the initially estimated dimensions are accurate, the object will be placed in the

container as planned. Otherwise, we re-run the TAP-Net++ using the updated dimensions and select the EMS entry with the highest score under the current box state constraint. This allows the robot to pack the already picked-up box into an optimal EMS location, without the complication of putting down the box and grabbing another box or another surface of the same box. This process repeats until no more source objects can be packed into the target container or the last packed object falls off due to unstable placement. In the latter scenario, the packing process for the current container is terminated prematurely, effectively penalizing the placement of objects in unstable locations.

Network training. We use the PPO algorithm [Schulman et al. 2017] to train our network due to the lack of data for supervision. To measure the final packing quality, we use compactness C as the reward function to guide the training. The compactness C is defined as the ratio between the total volume of packed boxes and the container volume. Intuitively, the compactness measure favors tightly-packed boxes and $C = 1$ if and only if the container is fully filled. If there are multiple target containers are used, we use the mean compactness of all the containers $C = \sum_{i=1}^{N_t} C_i / N_t$ as the reward function, where N_t is the number of containers used.

4 EXPERIMENTS

4.1 TAP-Benchmark

To thoroughly study the TAP problem and evaluate its solutions, we establish a benchmark consisting of multiple source box settings and target container settings, which have been motivated by different applications and usage scenarios; see Figure 6.

In more detail, there are three different settings for the source boxes with different levels of flexibility and difficulty:

- **FIX:** all source objects are sampled from a fixed set of N_f objects.
- **RAND:** the source object sizes have more variations and are randomly sampled from a given distribution.
- **PPSG:** short for Perfect Packing Solution Guaranteed, refers to a set of random boxes that are guaranteed to have a packing solution that can fully pack all the objects in one container, resulting in a perfect packing with $C = 1$. The data construction method is based on the bin packing problem generator [Laterre et al. 2018].



Fig. 6. Packing applications that roughly correspond to different target container settings.

There are two different settings for the target containers with different packing goals and constraints:

- **Single**: there is only a single target container and the goal is to fill the container with the source objects as fully as possible.
- **Multi**: a new empty target container can be added once the current container either runs out of space or is filled with unstable packing, and the goal is to pack all the source objects into the target containers. When there are multiple containers, we further subdivided the setting into two cases: **Multi-All** where all containers can be used to pack new objects, and **Multi-Last** where only the last added container can be used for future packing.

We set the target container size as $100 \times 100 \times 100$, and generate N_s source objects for packing, with the dimensions of each object being multiple of a unit length $u = 1$ and smaller than 100. For the *Single* container setting, we use the compactness C as the evaluation metric. For the *Multi* container setting, as multiple containers are used, we also add the container number N_t as an evaluation metric, along with compactness. Moreover, we further define the ideal container number for the set of source objects $\{O_i\}_{i=1}^{N_s}$ as $N_t^* = \lceil \sum_i V_i / V_t \rceil$, where V_i and V_t are the volumes of the object O_i and the target container, respectively, and use the extra number of containers used $\Delta N_t = N_t - N_t^*$ as an evaluation metric.

In the following experiments, we show results under different combinations of input-output settings as well as comparisons to baselines to show the robustness and generality of our method.

4.2 Baseline algorithms and comparisons

Baseline algorithms. We here compare our method to two baselines for object selection and packing optimization.

The first baseline is *TAP-Net* [Hu et al. 2020]. Using the same set of inputs as ours (box states, precedence graph, container height map), it outputs a valid packing sequence of box states. The packing position of each box state in the sequence is then computed using a greedy approach, i.e., the candidate EMS that yields the highest compactness for the box state is used.

The second baseline method referred to as *Greedy EMS*, considers all box states and candidate EMS extracted by our objects/container analysis. For each (oriented box, EMS) pair, the packing position is determined using the DBL corners as in our method. The pair that yields the highest compactness at each step is greedily selected.

To focus the evaluation on packing strategies, both baseline methods use the same source objects/container analysis and update objects/container states after each packing step. Moreover, for a fair evaluation, the object detection step is bypassed, since *TAP-Net* [Hu et al. 2020] requires a full observation of all the objects, with all the source objects axis-aligned with known sizes and blocking relations.

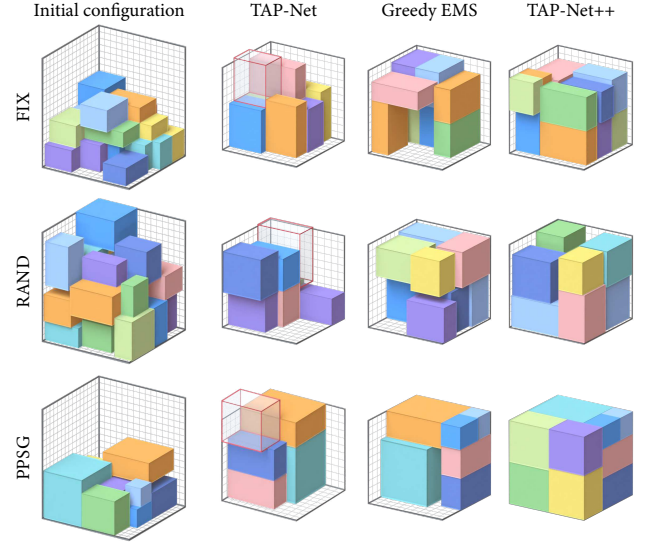


Fig. 7. Comparison of packing results between TAP-Net++ and two baseline methods under **Single** container setting. For each result obtained using TAP-Net, the box terminates the packing process is shown in transparent with a red frame, which is selected for packing in the current state but cannot fit into the target container using the heuristic packing strategy due to the height limit. Note that this box will not be counted for compactness calculation.

Table 2. Comparison on the performance of TAP-Net++ and two baseline methods under the **Single** container setting, with compactness C as the evaluation metric.

Method	FIX	RAND	PPSG
TAP-Net	0.379	0.345	0.564
Greedy EMS	0.500	0.514	0.764
TAP-Net++	0.657	0.656	0.929

We use $N_s = 20$ in the *FIX* and *RAND* source box setting comparisons, while for the *FIX* source box setting, we further specify $N_f = 5$, which means that the 20 objects are a random combination of 5 pre-determined objects. Moreover, for the *PPSG* source box setting, the boxes are constructed by splitting the space of one target container, so we set $N_s = 10$ to avoid getting too small boxes.

Comparison under *Single* container setting. Table 2 compares the performances of our network and the baseline methods when packing different groups of source objects into a *Single* target container. We can see that our method gets consistently better performance than those two baseline methods. The improvement varies from 20% to 30% when comparing TAP-Net++ to the *Greedy EMS* baseline. *TAP-Net* gets the worse results as it uses two-step optimization which selects the object states without simultaneously determining its packing location while both TAP-Net++ and the *Greedy EMS* baseline select the packing strategy in one step after constructing the candidate EMS packing location.

Table 3. Comparison on the performance of TAP-Net++ and two baseline methods under the **Multi-All** container setting.

Input type	Method	C	N_t	ΔN_t
FIX	TAP-Net	0.441	4.24	1.95
	Greedy EMS	0.430	4.34	2.05
	TAP-Net++	0.545	3.42	1.13
RAND	TAP-Net	0.427	4.36	2.18
	Greedy EMS	0.464	4.05	1.88
	TAP-Net++	0.538	3.49	1.32
PPSG	TAP-Net	0.478	2.13	1.13
	Greedy EMS	0.560	2.02	1.02
	TAP-Net++	0.761	1.49	0.48

Table 4. Comparison on the performance of TAP-Net++ and two baseline methods under the **Multi-Last** container setting.

Input type	Method	C	N_t	ΔN_t
FIX	TAP-Net	0.378	5.01	2.73
	Greedy EMS	0.361	5.20	2.91
	TAP-Net++	0.535	3.49	1.20
RAND	TAP-Net	0.343	5.39	3.22
	Greedy EMS	0.377	5.14	2.97
	TAP-Net++	0.540	3.46	1.28
PPSG	TAP-Net	0.455	2.27	1.27
	Greedy EMS	0.544	2.14	1.14
	TAP-Net++	0.731	1.54	0.54

Figure 7 shows some visual comparisons of the final packing results of different methods, demonstrating that TAP-Net++ provides more compact packing with more objects in the given container. In particular, considering the *PPSG* example illustrated in the last row, TAP-Net++ successfully identifies the optimal packing solution with a perfect compactness score of $C = 1$. The *Greedy EMS* approach selects suboptimal solutions throughout the process, resulting in narrow empty spaces that cannot accommodate the remaining objects. Furthermore, since TAP-Net does not explicitly extract candidate packing locations and mask out invalid pairs as the other two methods do, it failed to select the box state that can be properly packed into the container and terminates with the selection of the highlighted object in transparent.

Comparison under *Multi* container setting. Compared to the previous experiment, packing objects into *Multiple* containers is more challenging because more candidate packing locations need to be considered and longer-term planning needs to be performed to pack all the source objects into the target containers.

Table 3 and 4 compare the performances of our network and the baseline methods under *Multi-All* and *Multi-Last* container settings, respectively. They show that our method consistently yields better performance than the two baselines as in the *Single* setting. In addition, the packing performances under *Multi-All* are consistently better than those under *Multi-Last* because the former offers more flexible packing options and can make use of remaining free space in the previous containers. We have also observed that the advantage of

Table 5. Generality on box numbers N_s . When packing $N_s = \{20, 40, 60, 80, 100\}$ objects, the performance of TAP-Net++ trained on 20 objects is shown on the left column and that of TAP-Net++ trained on the same N_s objects is shown on the right.

N_s	Trained on 20 objects			Trained on N_s objects		
	C	N_t	ΔN_t	C	N_t	ΔN_t
20	0.540	3.46	1.28	0.540	3.46	1.28
40	0.556	6.62	2.53	0.583	6.30	2.21
60	0.550	10.03	4.05	0.586	9.39	3.42
80	0.540	13.59	5.78	0.582	12.60	4.79
100	0.542	16.97	7.33	0.575	15.96	6.32

our method is more pronounced in the *Multi-Last* setting compared to the *Multi-All* setting. We believe this is because *Multi-Last* poses a more constrained optimization problem, making it more challenging to achieve an optimal packing solution.

Figure 8 presents visual comparisons of results obtained by different methods for the same set of input objects packed under either the *Multi-All* or *Multi-Last* setting. It is evident that TAP-Net++ consistently achieves more compact packing results compared to the other methods. When comparing the results between the *Multi-All* and *Multi-Last* settings, particularly for TAP-Net and *Greedy EMS*, we can observe that the first container under the *Multi-All* setting is usually filled with more boxes than the first container under the *Multi-Last* setting in all three source settings (*PPSG*, *RAND*, and *FIX*). This difference arises due to the flexibility of packing all available containers in the *Multi-All* setting.

4.3 Generality of TAP-Net++

To evaluate the generality of TAP-Net++, we further test it under different object numbers and container sizes. Without loss of generality, we here focus the application of packing *RAND* source objects into multiple containers under the *Multi-Last* setting.

Generality on object number. The performance of neural networks often degenerates when the training and testing data have different characteristics. Since our approach uses a transformer encoder to encode precedence, it can handle an arbitrary number of input objects at the testing stage. Here we want to find out the impact of using different object numbers under training and testing stages. When testing the task of packing $N_s = \{20, 40, 60, 80, 100\}$ objects, two versions of TAP-Net++ are compared. The first version is trained using 20 objects, whereas the second is training using the same number of N_s objects. As shown in Table 5, the object number used for training TAP-Net++ has little impact on its performance. We also test the inference runtime performance with respect to the number of boxes. With an NVIDIA TITAN Xp, it takes consistently 20ms for TAP-Net++ to infer a \langle oriented box, EMS \rangle pair with different numbers of boxes. These suggest the robustness and generality of our method on box number.

Generality to container size. By default, we set the target container size as $100 \times 100 \times 100$. To test the generality of our method to the target container size, we directly apply our network trained on the default target container to two new container sizes: $150 \times 100 \times 100$

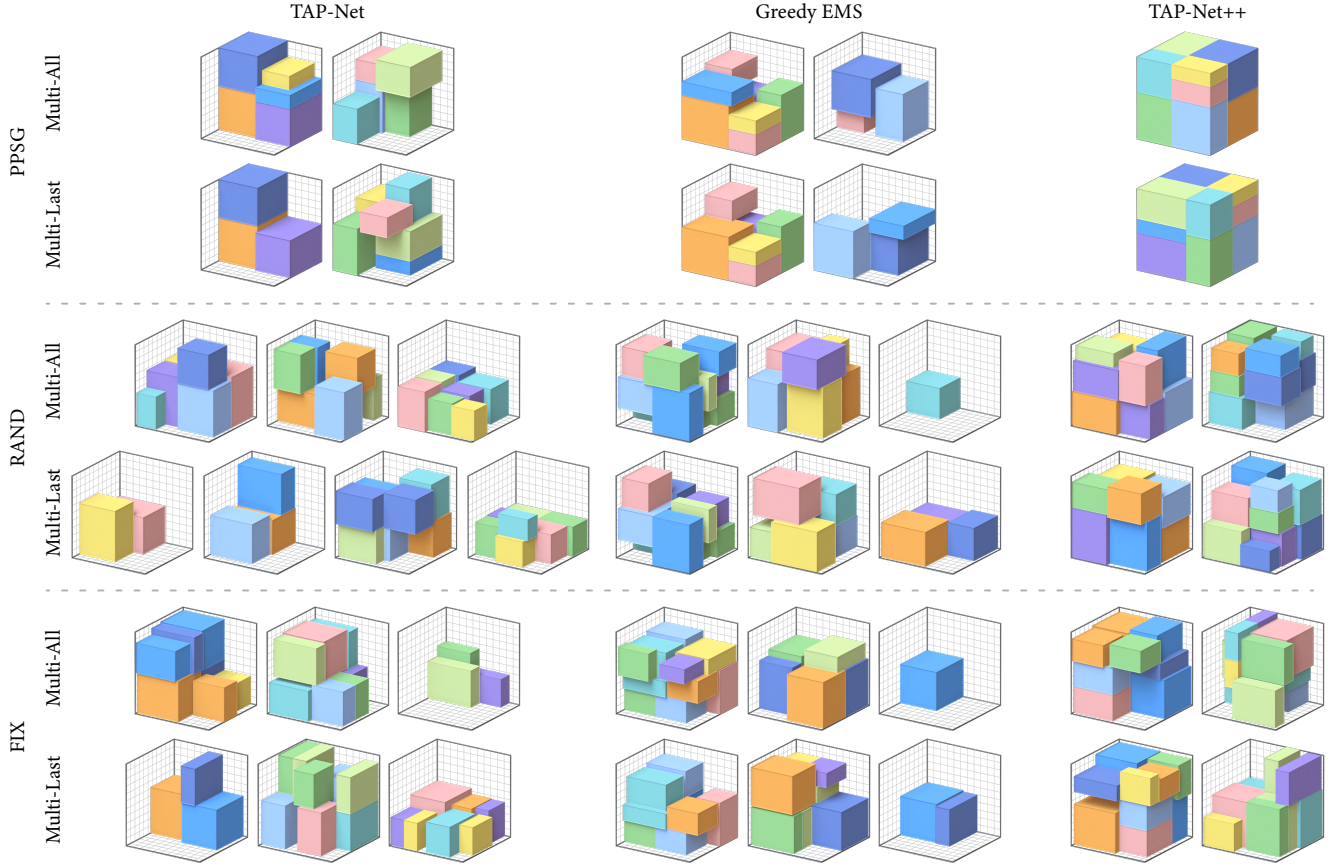


Fig. 8. Comparison of packing results between TAP-Net++ and two baseline methods under two **Multi** container settings. For each set of results under the same source setting, the input box configuration is the same but tested under either Multi-all or Multi-Last setting.

Table 6. Generality on container size. The networks (TAP-Net++ and greedy baseline) trained on target container size of $100 \times 100 \times 100$ is tested on different container sizes. TAP-Net++ has very stable performance, whereas greedy baseline uses 60% more containers when target container size changes.

Container size	TAP-Net++			Greedy EMS		
	C	N_t	ΔN_t	C	N_t	ΔN_t
$100 \times 100 \times 100$	0.540	3.46	1.28	0.377	5.14	2.97
$150 \times 100 \times 100$	0.554	3.31	1.20	0.286	6.77	4.65
$200 \times 100 \times 100$	0.542	3.42	1.32	0.235	8.34	6.25

and $200 \times 100 \times 100$. To make the evaluation metric comparable, the number of source objects are scaled accordingly to match target container size changes. The results are shown in Table 6, with the performance of *Greedy EMS* baseline included for comparison. We can see that the performance of our method is very stable, whereas that of the *Greedy EMS* baseline degenerates noticeably.

4.4 Results on causally stacked boxes

Thanks to our informative object information encoder and the generality of our network to the object number, the network we trained

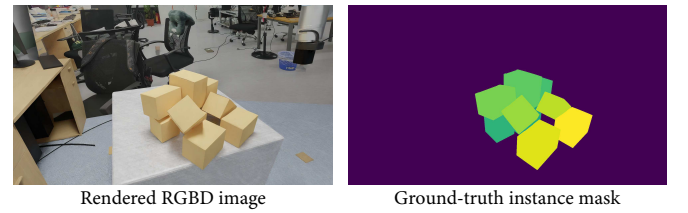


Fig. 9. Rendered images used to fine-tune the Mask RCNN network [He et al. 2017] for object detection in the real workspace.

on axis-aligned boxes with full observation can be directly used to deal with more practical settings with causally stacked boxes without the need for fine-tuning either in the simulator or in the real world.

Simulated environment. As shown in Figure 2(a & d), for each task, we generate N_s objects with random poses and let them fall onto a flat surface by gravity through pybullet simulator [Coumans and Bai 2016]. This provides the initial configuration for boxes, which are unknown to TAP-Net++. RGBD images are captured using a virtual camera to train Mask RCNN network [He et al. 2017] for

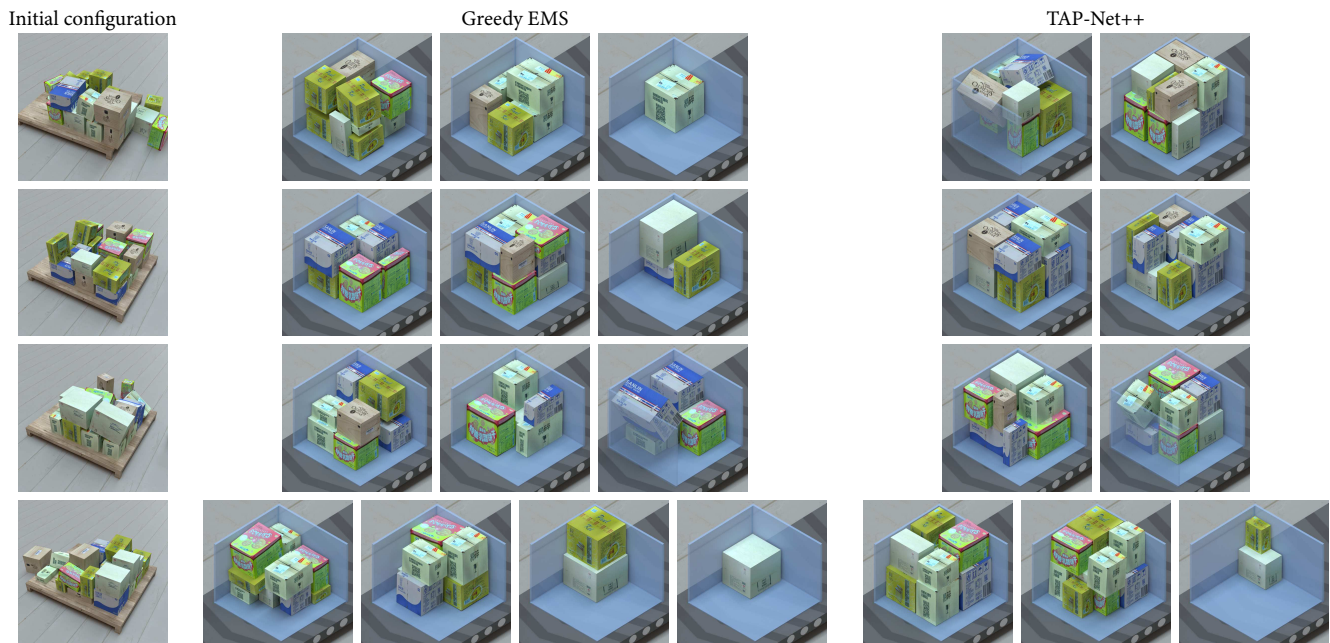


Fig. 10. Comparison of packing results between TAP-Net++ and the *Greedy EMS* baseline in a simulated environment where boxes are initially stacked casually, and their numbers and sizes are obtained through observations. Note that the container is not fully rendered to show the packed configuration more clearly.

Table 7. Comparison on the performance of the full pipeline (boxes with unknown sizes and numbers are initially stacked casually) obtained using TAP-Net++ and the *Greedy EMS* baseline method under the **RAND + Multi-Last** setting.

	C	N_t	ΔN_t
Greedy EMS	0.357	4.47	2.48
TAP-Net++	0.521	2.81	0.86

object extraction. Once the box shapes and their precedence are extracted, we apply TAP-Net++ trained on axis-aligned boxes with full observation to directly output the packing strategy. As TAP-Net cannot handle dynamic inputs, we only compare to the *Greedy EMS* baseline; see Table 7. We can see that our method performs much better than *Greedy EMS* and the results are similar to the results tested on the axis-aligned boxes with full observation.

Figure 10 shows visual comparisons of the final packing results of the two methods under this practical setting. For the input boxes casually stacked on the workspace as shown on the left, we found that the object detector can extract correct box sizes and locations for the following packing strategy optimization. Compared to the *Greedy EMS* baseline on the final packing results, our method successfully packs boxes into fewer containers with higher compactness.

Real world tests. Besides experiments in the simulated environment, we also validate our method using a real robot. The Mask RCNN network [He et al. 2017] is fine-tuned using rendered images of stacked objects with the real workspace setting as the background (see Figure 9), whereas the TAP-Net++ trained using synthesized

axis-aligned boxes is again applied directly in real tests without fine-tuning. Figure 1 shows several keyframes from one packing process.

Note that our approach may pick up objects from different sides, but always pack them into the container from the top. During the real execution, we enlarge the detected box sizes by a small amount before passing them to the TAP-Net++ to accommodate various errors of executing a packing plan in the real world, which may result in relatively loose packing compared to the simulated results.

We found that there are discrepancies in packing performance between the simulation and the real world. TAP-Net++ faces distinct complexities when executed in real-world scenarios compared to simulations mainly due to the inaccurate visual perception. The point clouds acquired by depth cameras in real-world scenarios often contain noises and distortions, and the Mask RCNN trained on rendered images may yield errors when applied to real images due to discrepancies between the virtual and actual environment. These factors result in potential inaccuracies in box size estimation and more frequently trigger the algorithm to re-plan placement than in simulation. Consequently, this might guide the packing strategy towards a sub-optimal solution instead of a globally optimal arrangement. Incorporating such stochastic placement events into our training process could potentially enhance the robustness and generalization of the algorithm.

Table 8. Ablation studies on precedence encoder used for source boxes.

Precedence encoder	C	N_t	ΔN_t
CNN	0.526	3.54	1.36
RNN	0.534	3.48	1.30
Transformer	0.540	3.46	1.28

Table 9. Ablation studies on the set of candidate EMS locations used.

Candidate locations	C	N_t	ΔN_t
Original EMS	0.526	3.52	1.35
Add constrained EMS	0.540	3.46	1.28

4.5 Ablation studies on network design

We now perform ablation studies on several key design choices. The application of packing *RAND* source objects into multiple containers under the *Multi-Last* setting is again used here.

Precedence encoder. In our workspace setting, the number of boxes detected varies at each step, and so is the size of the precedence matrix. We design a precedence encoder based on the transformer to handle this dynamic input size. Another choice would be the RNN, as it can handle dynamic input size as well. Since TAP-Net uses a CNN layer to encode the precedence matrix, it is also tested in this ablation study, even though its input size needs to be fixed.

The comparison of these three types of precedence encoders is shown in Table 8. It shows that our transformer-based encoder has the best performance. Although the performance of CNN is close when the input size is fixed, the transformer naturally supports dynamic input size and is more suitable in our setting.

Packing locations. Other than the original EMS, we added extra constrained EMS locations to provide more candidate packing locations for stable packing, as shown in Figure 4. Table 9 shows the quantitative comparisons. We can see that with extra constrained EMS locations effective candidate packing locations, better solutions can be found to increase performance. When checking the whole packing process, we indeed observe that compared to using the original EMS locations only, TAP-Net++ learns to select the constrained EMS where the boxes underneath can provide more stable support as long as it provides enough space.

Packing corners. Given a ⟨oriented box, EMS⟩ pair, TAP-Net++ always computes the packing location by aligning the DBL corners of both. It's possible to try aligning all four bottom corners and pick the best. Table 10 shows the performance comparison of using either one or four corners for packing location calculation. It shows that the performance of using the fixed DBL corner is slightly better than trying all four corners. Our hypothesis is that using a simple and consistent rule for packing location selection helps the network to focus on the optimization for ⟨oriented box, EMS⟩ pair. This hypothesis is supported by the observation that the network trained using four candidate corners eventually settles down with using the same corner for all EMS.

Feasibility mask. When taking stability into consideration, we found that only using the matching score to compute the relative

Table 10. Ablation studies on packing corner selection for box and location alignment.

Packing corners	C	N_t	ΔN_t
All four corners	0.523	3.56	1.38
DBL corner	0.540	3.46	1.28

Table 11. Ablation studies on the techniques used for avoiding unstable packing.

Method	C	N_t	ΔN_t
Matching score only	0.526	3.52	1.35
+ Unstable penalty	0.530	3.50	1.32
+ Feasibility mask	0.540	3.46	1.28

scores among different ⟨oriented box, EMS⟩ pairs is not enough to capture the stability of each individual pair well. Thus, we further compute a feasibility mask using the **sigmoid** operator after fusing the features to make the network learn the pair-wise properties better, and then combine the matching score and feasibility mask together to get the final output. We found that with the extra branch to predict the feasibility mask, TAP-Net learns to estimate the stability of each packing pair implicitly based on whether this selection increases the number of target containers and thus decreases the average compactness. Other than adding the feasibility mask to learn the information implicitly, we also tried guiding the network to learn stable packing by adding an instability penalty during training. Specifically, once an object is unstable, we add a new container and then add a penalty of -0.1 to our reward value. As shown in Table 11, compared to either directly encoding this information into the matching score or adding a direct penalty for unstable packing without introducing the extra feasibility mask, our current strategy obtained the best results over all evaluation metrics.

4.6 Generality on input without precedence

Our paper focuses more on the most challenging TAP problem setting with casually stacked and partially observed objects, where the precedence between the objects has to be taken into consideration. On the other hand, our method is sufficiently flexible to be directly used to deal with other application scenarios [Zhao et al. 2021b], where objects are lying on the conveyor belt for packing so that there is no precedence between objects. In this case, there may be m objects on the conveyor at the same time, each of which can only be picked up from the top with rotation only allowed around the z -axis, and the goal is to pack as many objects as possible into a given container. This is essentially the same as our *RAND + Single* setting, where each time, m objects are considered without precedence.

To show the generality of TAP-Net++ without object precedence, we present a comparison to the SOTA method PCT [Zhao et al. 2021b] under their experiment setting as explained above, where m is set to be 4, and the results are presented in Table 12. We can see that even though TAP-Net++ was not designed for this setting, it can still achieve slightly better performance than PCT, demonstrating the generality and practicality of our method.

Table 12. Comparison (compactness C) with PCT [Zhao et al. 2021b] under **RAND + Single** setting, each time considers 4 objects without precedence.

Method	RAND
PCT	0.663
TAP-Net++	0.669

5 CONCLUSION, LIMITATION, AND FUTURE WORK

We develop a learning framework for transport-and-packing using a robotic arm operating in a compact workspace. As the technical core, TAP-Net++ is trained with reinforcement learning; it takes both source box information and candidate packing locations derived from the target container as input and selects the optimal pair of box state and location to guide the full packing process. Extensive experiments have been conducted to demonstrate the superiority of our method over the state-of-the-art methods, confirm its generalization capability, and validate several of our key design choices.

One obvious limitation which can be attributed to the visual sensing step is that our method cannot process objects that are undetectable. It may be interesting to explore ways to discover unknown objects using the dynamic visual data captured during the packing process. Moreover, when applying our method in the real-world test, we currently perform fine-tuning of the object detection network using images captured from a camera positioned above the workspace. While we believe that this is a reasonable requirement considering the fixed nature of the workspace setup, further investigations are needed to explore methods for making the object detection network adaptive to different setups.

Furthermore, the inaccuracies arising from object detection and box dimension estimation could lead to more frequent local packing strategy adjustments once an object is picked up and resulting in potentially sub-optimal solutions. Hence, aside from improving the accuracies, it would also be interesting to incorporate the ensuing uncertainties into the input encoding and enhance the policy learning or add a buffer zone to avoid forced packing.

Last but not least, it is worth exploring ways to optimize low-level control of the robot arm directly through reinforcement learning instead of relying on an existing motion planning method so that the movement paths and packing stability can be simultaneously considered together with compactness.

ACKNOWLEDGMENTS

We thank the anonymous reviewers for their valuable comments. Thanks are also extended to Jiahui Zhu and Xueqi Ma for their help. This work was supported in part by NSFC (62322207, U2001206, 62161146005, U21B2023), Guangdong Natural Science Foundation (2021B1515020085), Shenzhen Science and Technology Program (RCYX20210609103121030), DEGP Innovation Team (2022KCXTD025), NSERC (No. 611370, 2023-05035), gift funds from Adobe, and Guangdong Laboratory of Artificial Intelligence and Digital Economy (SZ).

REFERENCES

- Mauro Maria Baldi, Teodor Gabriel Crainic, Guido Perboli, and Roberto Tadei. 2012. The generalized bin packing problem. *Transportation Research Part E: Logistics and Transportation Review* 48, 6 (2012), 1205–1220.

- Xuelin Chen, Hao Zhang, Jinjie Lin, Ruizhen Hu, Lin Lu, Qi xing Huang, Bedrich Benes, Daniel Cohen-Or, and Baoquan Chen. 2015. Dapper: Decompose-and-Pack for 3D Printing. *ACM Transactions on Graphics (TOG)* 34, 6 (2015), Article 213.
- Erwin Coumans and Yunfei Bai. 2016. Pybullet, a python module for physics simulation for games, robotics and machine learning. (2016).
- Teodor Gabriel Crainic, Guido Perboli, and Roberto Tadei. 2008. Extreme point-based heuristics for three-dimensional bin packing. *Inform. Journal on computing* 20, 3 (2008), 368–384.
- Lars Doyle, Forest Anderson, Ehren Choy, and David Mould. 2019. Automated pebble mosaic stylization of images. *Computational Visual Media* 5, 1 (2019), 33–44.
- Chi Trung Ha, Trung Thanh Nguyen, Lam Thu Bui, and Ran Wang. 2017. An online packing heuristic for the three-dimensional container loading problem in dynamic environments and the Physical Internet. In *European Conference on the Applications of Evolutionary Computation*. Springer, 140–155.
- Kaiming He, Georgia Gkioxari, Piotr Dollár, and Ross Girshick. 2017. Mask r-cnn. In *Proceedings of the IEEE international conference on computer vision*. 2961–2969.
- Haoyuan Hu, Xiaodong Zhang, Xiaowei Yan, Longfei Wang, and Yinghui Xu. 2017. Solving a new 3d bin packing problem with deep reinforcement learning method. *arXiv preprint arXiv:1708.05930* (2017).
- Ruizhen Hu, Juzhan Xu, Bin Chen, Minglun Gong, Hao Zhang, and Hui Huang. 2020. TAP-Net: transport-and-pack using reinforcement learning. *ACM Transactions on Graphics (SIGGRAPH Asia)* 39, 6 (2020), 1–15.
- Hao Jiang and Jianxiong Xiao. 2013. A linear approach to matching cuboids in RGBD images. In *Proceedings of the IEEE conference on computer vision and pattern recognition*. 2171–2178.
- Craig S Kaplan and David H Salesin. 2000. Escherization. In *Proceedings of the 27th annual conference on Computer graphics and interactive techniques*. 499–510.
- Korhan Karabulut and Mustafa Murat Inceoglu. 2004. A hybrid genetic algorithm for packing in 3D with deepest bottom left with fill method. In *International Conference on Advances in Information Systems*. Springer, 441–450.
- Bongjin Koo, Jean Hergel, Sylvain Lefebvre, and Niloy J Mitra. 2016. Towards zero-waste furniture design. *IEEE transactions on visualization and computer graphics* 23, 12 (2016), 2627–2640.
- Alexandre Laterre, Yunguan Fu, Mohamed Khalil Jabri, Alain-Sam Cohen, David Kas, Karl Hajjar, Torbjorn S Dahl, Amine Kerkeni, and Karim Beguir. 2018. Ranked reward: Enabling self-play reinforcement learning for combinatorial optimization. *arXiv preprint arXiv:1807.01672* (2018).
- Bruno Lévy, Sylvain Petitjean, Nicolas Ray, and Jérôme Mailliot. 2002. Least squares conformal maps for automatic texture atlas generation. In *ACM transactions on graphics (TOG)*, Vol. 21. ACM, 362–371.
- Xueping Li and Kaike Zhang. 2015. A hybrid differential evolution algorithm for multiple container loading problem with heterogeneous containers. *Computers & Industrial Engineering* 90 (2015), 305–313.
- Max Limper, Nicholas Vining, and Alla Sheffer. 2018. BoxCutter: Atlas Refinement for Efficient Packing via Void Elimination. *ACM Transactions on Graphics (TOG)* 37, 4 (2018).
- Andrea Lodi, Silvano Martello, and Daniele Vigo. 2002. Heuristic algorithms for the three-dimensional bin packing problem. *European Journal of Operational Research* 141, 2 (2002), 410–420.
- Silvano Martello, David Pisinger, and Daniele Vigo. 2000. The three-dimensional bin packing problem. *Operations research* 48, 2 (2000), 256–267.
- Silvano Martello, David Pisinger, Daniele Vigo, Edgar Den Boef, and Jan Korst. 2007. Algorithm 864: General and robot-packable variants of the three-dimensional bin packing problem. *ACM Transactions on Mathematical Software (TOMS)* 33, 1 (2007), 7–es.
- Tobias Nöll and Didier Stricker. 2011. Efficient Packing of Arbitrarily Shaped Charts for Automatic Texture Atlas Generation. In *Proc. of Eurographics Conference on Rendering (EGSR)*. 1309–1317.
- Francisco Parreño, Ramón Alvarez-Valdés, Jose Manuel Tamarit, and Jose Fernando Oliveira. 2008. A maximal-space algorithm for the container loading problem. *INFORMS Journal on Computing* 20, 3 (2008), 412–422.
- Pedro V Sander, Zoë J Wood, Steven Gortler, John Snyder, and Hugues Hoppe. 2003. Multi-chart geometry images. (2003).
- John Schulman, Filip Wolski, Prafulla Dhariwal, Alec Radford, and Oleg Klimov. 2017. Proximal policy optimization algorithms. *arXiv preprint arXiv:1707.06347* (2017).
- Juraj Vanek, JA Garcia Galicia, Bedrich Benes, R Méch, N Carr, Ondrej Stava, and GS Miller. 2014. PackMerger: A 3D print volume optimizer. In *Computer Graphics Forum*, Vol. 33. Wiley Online Library, 322–332.
- Fan Wang and Kris Hauser. 2019. Stable bin packing of non-convex 3D objects with a robot manipulator. (2019), 8698–8704.
- Hang Zhao, Qijin She, Chenyang Zhu, Yin Yang, and Kai Xu. 2021a. Online 3D bin packing with constrained deep reinforcement learning. In *Proceedings of the AAAI Conference on Artificial Intelligence*, Vol. 35. 741–749.
- Hang Zhao, Yang Yu, and Kai Xu. 2021b. Learning Efficient Online 3D Bin Packing on Packing Configuration Trees. In *International Conference on Learning Representations*.